Modern Physics Letters B
Vol. 27, No. 25 (2013) 1350184 (12 pages)

DOI: 10.1142/S0217984913501844

World Scientific
www.worldscientific.com

PARAMETRIC EXCITATION OF SOLITONS IN DIPOLAR BOSE–EINSTEIN CONDENSATES

A. BENSEGHIR* and W. A. T. WAN ABDULLAH†

Department of Physics, Faculty of Science, University of Malaya, Malaysia
**benseghir1@yahoo.com*
†*wat@um.edu.my*

B. A. UMAROV

Faculty of Science, International Islamic University Malaysia,
Jalan Sultan Ahmad Shah, 25200 Kuantan, Pahang, Malaysia
bakhram@iium.edu.my

B. B. BAIZAKOV

Physical-Technical Institute, Uzbek Academy of Sciences,
Tashkent 100084, Uzbekistan
baizakov@uzsci.net

Received 13 June 2013
Revised 28 July 2013
Accepted 29 July 2013
Published 19 September 2013

In this paper, we study the response of a Bose–Einstein condensate with strong dipole–dipole atomic interactions to periodically varying perturbation. The dynamics is governed by the Gross–Pitaevskii equation with additional nonlinear term, corresponding to a nonlocal dipolar interactions. The mathematical model, based on the variational approximation, has been developed and applied to parametric excitation of the condensate due to periodically varying coefficient of nonlocal nonlinearity. The model predicts the waveform of solitons in dipolar condensates and describes their small amplitude dynamics quite accurately. Theoretical predictions are verified by numerical simulations of the nonlocal Gross–Pitaevskii equation and good agreement between them is found. The results can lead to better understanding of the properties of ultra-cold quantum gases, such as ^{52}Cr, ^{164}Dy and ^{168}Er, where the long-range dipolar atomic interactions dominate the usual contact interactions.

Keywords: Bose–Einstein condensate; dipolar interactions; matter-wave soliton; shape oscillations; variational approach.

1. Introduction

The properties of cold quantum gases are mainly determined by interaction forces between particles. For dilute gases of alkali atoms, which constitute the major part of the Bose–Einstein condensates (BEC) family, interaction potential in the ultra-

cold regime can be modeled, to a very good precision, by a delta function $U_{\rm cont}(\mathbf{r}) = 4\pi\hbar^2 m^{-1} a_s \cdot \delta(\mathbf{r})$. This corresponds to isotropic contact interaction between particles of mass m, whose strength is proportional to the s-wave atomic scattering length a_s. Such a single parameter pseudo-potential has been quite successful in interpretation of experimental data obtained in the mean field regime.[1,2]

Bose–Einstein condensation of chromium with anisotropic and long-range dipolar atomic interactions has opened new direction in the physics of ultra-cold quantum gases.[3,4] Subsequently, two other species with strong dipolar interactions, namely dysprosium[5] and erbium,[6] were Bose condensed. The principal difference of chromium condensates from the alkali atom condensates is that, ^{52}Cr has a large permanent magnetic dipole moment $\mu = 6\mu_B$, where $\mu_B = e\hbar/2m_e$ is the Bohr magneton. Since the dipole–dipole force is proportional to the square of the magnetic moment, the dipolar interactions in chromium condensate is a factor of 36 times stronger than in alkali atom condensates, like ^{87}Rb. Similar arguments pertain also for other dipolar quantum gases, ^{164}Dy and ^{168}Er. There is another group of alkaline-earth elements ^{40}Ca and ^{84}Sr, Bose-condensation of which was reported in Refs. 7 and 8, respectively, which do not carry the magnetic moment. The peculiarity of this group is that, the condensate can be held and manipulated in optical traps. In addition, magnetic Feshbach resonances, frequently applied to tune the scattering properties of other atomic systems, are absent here. The optical Feshbach resonance technique,[9] instead of magnetic, serves the purpose in BEC of alkaline-earth elements. This group holds promise for wide applications in metrology, quantum computation, quantum simulators of many-body phenomena and ultracold plasmas.

Long-range and anisotropic character of atomic interactions drastically modify the properties of dipolar condensates compared to other BECs that have been created so far.[10] Tunability of contact interactions by a Feshbach resonance[11] allows to enter the regime of dominant dipolar interactions by lowering the contact interactions. In fact continuous transition between both regimes, with dominant contact or long range interactions is possible by this technique.

Interactions between atoms in BEC is the factor leading to nonlinearity of the governing equation. Although these interactions are very weak in dilute gases, all essential properties of BECs are determined by the strength, range and symmetry of interatomic forces. For short range contact interactions and sufficiently low temperature, the dynamics of BEC is well described by the Gross–Pitaevskii equation (GPE) with local cubic nonlinearity.[12,13] In contrast to other elements in the BEC family, the atomic interactions in dipolar gases are long-range and anisotropic. This circumstance substantially changes the properties and mathematical treatment of dipolar BECs. Due to the long-range correlations, not only the local density but also the whole density distribution in the condensate determines the interaction potential of an atom in the cloud. In its turn this leads to the nonlocal GPE for description of the dynamics of dipolar condensates.

The nonlocal character of atomic interactions prevents collapse of a two-dimensional (2D) BEC loaded in a pancake-shaped trap and gives rise to stable isotropic[14] and anisotropic 2D solitons,[15] whose properties are well described by the variational approximation (VA). Some essential properties of 1D bright solitons in dipolar BEC with competing local and nonlocal atomic interactions, including the existence regimes, stability and collision dynamics, were reported in Ref. 16. Recently a model for the dipolar condensate has been introduced, in which the dipole–dipole interaction is periodically modulated in space.[17] It was shown that the VA provides accurate predictions for the shape of solitons and their stability by means of the Vakhitov–Kolokolov criterion. The importance of low energy shape oscillations of matter-wave packets in studies of microscopic properties of dipolar quantum gases was pointed out in Ref. 18. A nonintegral form of the GPE for polarized molecules was proposed in Ref. 19 and applied to investigation of the collective excitation spectrum of dipolar BEC. The existence regime of bright solitons in the electrically polarized BEC was identified using the proposed model.

The objective of this work is to study the dynamics of a dipolar BEC governed by the nonlocal GPE by means of variational approximation[20] and numerical simulations. Recently, similar approach has been applied to interaction of a soliton with a weak potential barrier in the middle of the parabolic trap.[21] Our work distinguishes itself from other relevant publications in that, we obtain explicit ordinary differential equation for parameters of the soliton, instead of integro-differential equations, involving special functions. Also, we provide thorough comparison between the results of VA and numerical simulations of the GPE.

The paper is organized as follows. In Sec. 2, we briefly describe the potential of dipolar interactions between atoms and introduce the nonlocal GP equation. In Sec. 3, the VA for the nonlocal GPE has been developed and applied to low energy shape oscillations of the condensate. In concluding Sec. 4, we summarize our findings.

2. The Interaction Potential and Governing Equation

Atomic density in dilute quantum gases is in the range $\sim 10^{13} - 10^{15}$ cm^{-3}, which is four to six orders of magnitude smaller than the molecular density in air at room temperature and normal atmospheric pressure $\sim 10^{19}$ cm^{-3}. Despite the extremely low atomic density of BECs, their properties are strongly influenced by interatomic interactions. In ultra-cold quantum gases without significant magnetic or electric dipole moments, usually only short-range, isotropic contact interactions are important.

When atoms have significant dipole moment a new kind of interaction via long-range and anisotropic dipolar forces arises, in addition to contact interactions. The corresponding potential of dipole–dipole interactions is[4]

$$U_{dd}(r,\theta) = \frac{C_{dd}}{4\pi}\frac{1-3\cos(2\theta)}{r^3}\,, \tag{1}$$

where the coupling constant $C_{dd} = \mu_0\mu^2$ for atoms having permanent magnetic dipole moment μ (μ_0 is the permeability of vacuum), and $C_{dd} = d^2/\epsilon_0$ for atoms having permanent electric dipole moment d (ϵ_0 is the permittivity of vacuum), θ is the angle between the direction joining the two dipoles, and the orientation of the dipoles (here we assumed that all dipoles are aligned along the same direction). It should be pointed out that electric dipole moment can also be induced by exposing the gas to DC electric fields.[22]

It is evident from Eq. (1) that dipolar interactions are anisotropic — for instance, two dipoles placed head-to-tail ($\theta = 0$) attract each other, while placed side-by-side ($\theta = \pi/2$) repel. Tuning the strength of dipolar interaction is also possible by fast rotation of the orientation of dipoles in the polarizing field.[23] The time averaged potential has the form:[4]

$$\langle U_{dd}(r,\theta,\phi)\rangle = \frac{\mu_0\mu^2}{4\pi}\frac{1-3\cos(2\theta)}{r^3}\left[\frac{3\cos^2(\phi)-1}{2}\right]. \tag{2}$$

When the tilt angle changes in the interval $\phi \in [0, \pi/2]$ the term in the rectangular brackets changes from 1 to $-1/2$.

In real experimental conditions, there is always a competition between the dipolar and contact interactions. A dimensionless coefficient, characterizing the relative strength of these two kinds of atomic forces has been introduced:[4]

$$\varepsilon_{dd} = \frac{\mu_0\mu^2 m}{12\pi\hbar^2 a_s}, \tag{3}$$

where the numerical factors are chosen in such a way that, the homogeneous condensate is stable against 3D collapse, when $\varepsilon_{dd} < 1$. In particular, for ^{52}Cr atoms with the s-wave scattering length $a_s = 16a_B$ and magnetic dipole moment $\mu = 6\mu_B$, where a_B and μ_B are the Bohr radius and the Bohr magneton, respectively, one has $\varepsilon_{dd} = 0.16$. This can be compared to the ordinary case of ^{87}Rb atoms with $a_s = 0.7a_B$ and $\mu = 1.0\mu_B$, when the calculation gives $\varepsilon_{dd} = 0.007$. Therefore, the effect of dipolar interactions in ^{52}Cr condensate is much stronger than in ^{87}Rb condensate.

The GPE for the wave function of a dipolar condensate has the form:[24]

$$i\hbar\frac{\partial\Psi}{\partial t} = -\frac{\hbar^2}{2m}\Delta\Psi + \left[V_{\text{ext}}(\mathbf{r}) + \frac{4\pi\hbar^2 a_s}{m}|\Psi|^2 + \int U_{dd}(\mathbf{r}-\mathbf{r}',t)|\Psi(\mathbf{r}',t)|^2 d\mathbf{r}'\right]\Psi, \tag{4}$$

where $V_{\text{ext}}(\mathbf{r})$ is the external trapping potential for the condensate.

In this paper, we shall consider the dynamics of a dipolar condensate in quasi-1D geometry. Experimentally this setting can be realized by loading the condensate in a cigar shaped trap with tight radial confinement and weak axial confinement. The dipoles are assumed to be aligned along the axial x-direction, therefore the dipolar interaction is attractive. When the radial confinement is strong enough, one can assume that the radial dynamics is frozen and factorize the wave function as $\Psi(x,\rho,t) = \psi(x,t)\phi(\rho)$, where $\phi(\rho) = \exp(-\rho^2/2l^2)/\sqrt{\pi}l$ is the ground state of

a 2D harmonic oscillator with $l = \sqrt{\hbar/m\omega_\perp}$ being the radial harmonic oscillator length, $\omega_\perp$ is the radial trap frequency. Inserting the above factorized wave function into Eq. (4) and performing integration with respect to variable ρ, the following reduced 1D GPE can be obtained:

$$i\hbar\frac{\partial\psi}{\partial t} = -\frac{\hbar^2}{2m}\frac{\partial^2\psi}{\partial x^2} + \left(V_{\rm ext}(x) + g_{1D}|\psi|^2 + \int_{-\infty}^{+\infty} U_{dd}(|x-\xi|)|\psi(\xi,t)|^2 d\xi\right)\psi\,, \tag{5}$$

where $g_{1D} = 2\hbar\omega a_s$ is the reduced 1D nonlinear coupling constant, $V_{\rm ext}(x) = (1/2)m\omega^2 x^2$ is axially confining potential (parabolic trap with frequency ω). The reduced 1D potential of dipolar interactions was derived in[25]

$$U_{dd}(x) = -\frac{2\alpha d^2}{l^3}\left[2|x| - \sqrt{\pi}(1+2x^2)\exp(x^2)\,{\rm erfc}(|x|)\right], \tag{6}$$

where d is the dipole moment, l is the harmonic oscillator length of strong radial confinement, α is a variable that may change between $\alpha = 1$ ($\theta = 0$) and $\alpha = -1/2$ ($\theta = \pi/2$). Note that although the original 3D potential of dipole–dipole interactions is singular at $r = 0$, the reduced 1D potential is regularized and finite at $x = 0$. Equation (5) can be further reduced to dimensionless form by introducing variables: $x \to x/l$, $t \to \omega t$, $\psi \to \sqrt{2a_s}\psi$, $d \to d/\sqrt{(l^3\hbar\omega)}$

$$i\frac{\partial\psi}{\partial t} = -\frac{1}{2}\frac{\partial^2\psi}{\partial x^2} + \left(V_{\rm ext}(x) - q|\psi|^2 - 2\alpha d^2\int_{-\infty}^{+\infty} R(|x-\xi|)|\psi(\xi,t)|^2 d\xi\right)\psi\,, \tag{7}$$

where $R(x) \sim U_{dd}(x)$ is the dimensionless nonlocal kernel function, and $q \sim -{\rm sgn}(a_s)$ is the dimensionless strength of contact interactions.

Equation (7) in absence of external potential and nonlocal integral term is the well known 1D nonlinear Schrödinger equation, which supports a spectrum of exact soliton solutions. In experiments, one approaches this limit by confining the condensate in an elongated cigar shaped trap with tight radial confinement. Although the presence of a weak axial trap $V_{\rm ext}(x)$ breaks the integrability of the governing equation, many properties of localized states remain close to those of the classical solitons, as demonstrated in the recent experiment.[26] The nonlocal term in Eq. (7) also breaks the integrability, but it does not exclude the existence of stable localized states in the system in particular regions of the parameter space.[16] Since we are mainly interested in self-trapped localized states of BEC, for our purposes the external trap potential can be set to zero $V_{\rm ext}(x) = 0$, and this will be assumed below. It should be pointed out, that the external potential can be easily incorporated into the scheme of VA.[20]

Thus, when the dipolar atomic interactions are taken into account, the equation governing the dynamics of the condensate is the nonlocal GPE (7). Both the contact interactions represented in this equation by the cubic nonlinearity, and dipolar interactions represented by the integral term, are tunable by the Feshbach resonance technique. We shall be interested in periodic variation of the dipolar interactions at fixed strength of contact interactions.

3. The Variational Approximation

Below we consider the following equation describing the dynamics of the condensate in presence of both dipolar and contact interactions:

$$i\frac{\partial\psi}{\partial t}+\frac{1}{2}\frac{\partial^2\psi}{\partial x^2}+q|\psi|^2\psi+g(t)\psi\int_{-\infty}^{+\infty}R(|x-\xi|)\,|\psi(\xi,t)|^2d\xi=0\,, \tag{8}$$

where $g(t)=2\alpha(t)d^2$ is the strength of dipolar interactions, which can be varied through time dependent α. The wave function $\psi(x,t)$ is normalized to $N=\int_{-\infty}^{+\infty}|\psi(x)|^2dx$, which is a conserved quantity of Eq. (8), proportional to the number of atoms in the condensate.

The kernel function (6) is complicated for the variational analysis. For qualitative understanding of the effect of nonlocality on the dynamics of dipolar BEC we consider analytically tractable Gaussian ansatz for the response function:

$$R(x)=\frac{1}{\sqrt{2\pi}w}\exp\left(-\frac{x^2}{2w^2}\right)\,, \tag{9}$$

which is normalized to one $\int_{-\infty}^{+\infty}R(x)dx=1$, and Gaussian ansatz:

$$\psi(x,t)=A(t)\exp\left[-\frac{x^2}{2a(t)^2}+ib(t)x^2+i\phi(t)\right]\,, \tag{10}$$

with norm $N=\int|\psi(x)|^2dx=A^2a\sqrt{\pi}$.

Equation (8) can be derived from the Lagrangian density

$$\mathcal{L}=\frac{i}{2}(\psi\psi_t^*-\psi^*\psi_t)+\frac{1}{2}|\psi_x|^2-\frac{1}{2}q|\psi|^4-\frac{1}{2}g(t)|\psi(x,t)|^2\int_{-\infty}^{\infty}R(x-\xi)|\psi(\xi,t)|^2d\xi\,, \tag{11}$$

where the subscript denotes derivative with respect to corresponding variable, i.e. $\psi_t=\partial\psi/\partial t$, $\psi_x=\partial\psi/\partial x$. Now using the trial function (10) one obtains

$$\mathcal{L}_1=\frac{i}{2}(\psi\psi_t^*-\psi^*\psi_t)=A^2e^{-x^2/a^2}(b_tx^2+\phi_t)\,, \tag{12}$$

$$\mathcal{L}_2=\frac{1}{2}|\psi_x|^2=\frac{1}{2}A^2\left(\frac{1}{a^4}+4b^2\right)x^2e^{-x^2/a^2}\,, \tag{13}$$

$$\mathcal{L}_3=-\frac{1}{2}q|\psi|^4=-\frac{1}{2}qA^4e^{-2x^2/a^2}\,, \tag{14}$$

$$\begin{aligned}\mathcal{L}_4&=-\frac{1}{2}g(t)|\psi|^2\int_{-\infty}^{\infty}R(x-\xi)|\psi(\xi,t)|^2d\xi\\&=-\frac{g(t)A^4}{2\sqrt{2\pi}w}\int_{-\infty}^{\infty}\exp\left[-\frac{(x-\xi)^2}{2w^2}\right]\exp\left[-\frac{x^2+\xi^2}{a^2}\right]d\xi\,.\end{aligned} \tag{15}$$

To evaluate the last integral in $\mathcal{L}_4$ we make the change of variables[21] $z=\frac{1}{2}(x-\xi)$, $y=\frac{1}{2}(x+\xi)$, therefore $x=y+z$, $\xi=y-z$, i.e. we have functional dependence between old and new variables $x=x(y,z)$, $\xi=\xi(y,z)$. Then for the Jacobian of

the transformation we have $J = |x_y\xi_z - x_z\xi_y| = 2$. Consequently $dxd\xi = 2dydz$. The averaged Lagrangian terms $L_i = \int \mathcal{L}_i dx$ are computed straightforwardly

$$L_1 = A^2 a\sqrt{\pi}\left(\frac{1}{2}a^2 b_t + \phi_t\right), \tag{16}$$

$$L_2 = A^2 a\sqrt{\pi}\left(\frac{1}{4a^2} + a^2 b^2\right), \tag{17}$$

$$L_3 = -\frac{qA^4\sqrt{\pi}a}{2\sqrt{2}}, \tag{18}$$

$$\begin{aligned} L_4 &= -\frac{g(t)A^4}{\sqrt{2\pi}w}\int_{-\infty}^{+\infty}\int_{-\infty}^{+\infty}\exp\left[-\frac{2z^2}{w^2}\right]\exp\left[-\frac{2(y^2+z^2)}{a^2}\right]dydz \\ &= -\frac{g(t)A^4 a^2\sqrt{\pi}}{2\sqrt{2}\sqrt{a^2+w^2}}. \end{aligned} \tag{19}$$

Then the final expression for the averaged Lagrangian $L = L_1 + L_2 + L_3 + L_4$ is

$$\frac{L}{N} = \frac{1}{4a^2} + a^2 b^2 + \frac{1}{2}a^2 b_t + \phi_t - \frac{qN}{2\sqrt{2\pi}a} - \frac{g(t)N}{2\sqrt{2\pi}(a^2+w^2)^{1/2}}. \tag{20}$$

The Euler–Lagrange equations $d/dt(\partial L/\partial\nu_t) - \partial L/\partial\nu = 0$ for variational parameters $\nu \to \phi, b, a$ yield the following system:

$$N_t = 0, \quad a_t = 2ab, \quad b_t = \frac{1}{2a^4} - 2b^2 - \frac{qN}{2\sqrt{2\pi}a^3} - \frac{g(t)N}{2\sqrt{2\pi}(a^2+w^2)^{3/2}}. \tag{21}$$

The first equation in (21) is decoupled from others and declares the conservation of the wave packet's norm. The equation for the width of the soliton can be derived from the last two equations in (21):

$$a_{tt} = \frac{1}{a^3} - \frac{qN}{\sqrt{2\pi}a^2} - \frac{g(t)N}{\sqrt{2\pi}}\frac{a}{(a^2+w^2)^{3/2}}. \tag{22}$$

This equation is similar to equation of motion for a unit mass particle in the anharmonic potential

$$a_{tt} = -\frac{\partial U}{\partial a}, \quad \text{with} \quad U(a) = \frac{1}{2a^2} - \frac{qN}{\sqrt{2\pi}a} - \frac{gN}{\sqrt{2\pi}(a^2+w^2)^{1/2}}. \tag{23}$$

The stationary state corresponding to the minimum of the potential well $\partial U/\partial a = 0$ gives the width of the soliton and its amplitude via the norm $A = \sqrt{N/(a\sqrt{\pi})}$. Therefore, the shape of the soliton, given by Eq. (10) is determined by the variational approximation.

Equation (22) which allows to find the stationary solution of the original GPE (8) and describes its dynamics near the fixed point, is the main result of the present work. At large departures from the stationary state, the waveform (10) can deviate from the Gaussian shape, and the predictions of the VA become less accurate.

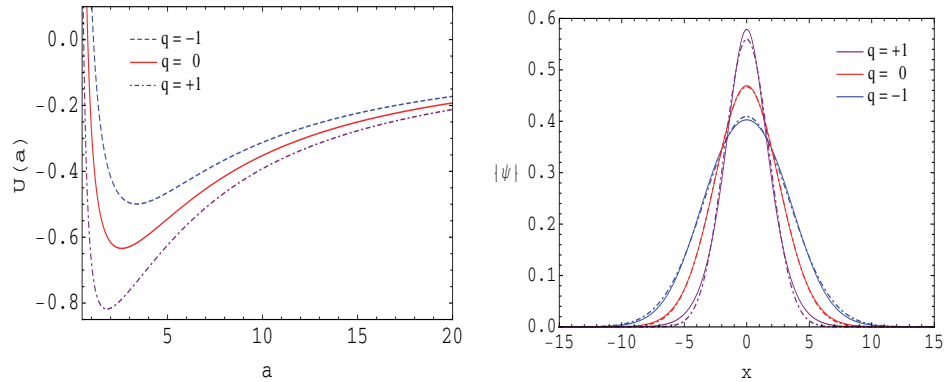

Fig. 1. (Color online) Left panel: The shape of the anharmonic potential given by Eq. (23) for pure dipole–dipole interactions ($q = 0$, red solid line), and in presence of repulsive ($q = -1$, blue dashed line) and attractive ($q = +1$, purple dot-dashed line) contact interactions. The stationary width of the soliton corresponding to these cases are $a_0 = 2.59$, $a_0 = 3.37$ and $a_0 = 1.80$, respectively. Right panel: Stationary localized solutions of the GPE (8) with Gaussian response function (9) for pure dipolar interactions (red line) and in presence of repulsive (blue line) and attractive (purple line) contact interactions. Dashed lines correspond to predictions of the VA. Parameter values: $N = 1$, $w = 5.0$ and $g = 10$.

The stationary width of the soliton a_0 is calculated from the following condition:

$$\frac{a_0^4}{(a_0^2 + w^3)^{3/2}} + \frac{q}{g} a_0 - \frac{\sqrt{2\pi}}{gN} = 0\,. \tag{24}$$

Figure 1 illustrates the shape of the potential $U(a)$ for a pure dipolar condensate ($q = 0$), and when the contact interactions are also present ($q = \pm 1$). The stationary state solutions of the GPE for these cases are obtained by the method of relaxation in imaginary time, as described in Ref. 27. As can be seen from this figure, the soliton in a pure dipolar condensate ($q = 0$) is perfectly described by the Gaussian function. The result of numerical solution of the GPE is indistinguishable from the prediction of VA. In presence of contact interactions ($q = \pm 1$), noticeable deviation from the Gaussian shape is seen near the peak and periphery of the wave packet.

The frequency of small amplitude oscillations around the fixed point a_0 is

$$\omega_0 = \left[\frac{3}{a_0^4} - \frac{2qN}{\sqrt{2\pi} a_0^3} - \frac{gN}{\sqrt{2\pi}(a_0^2 + w^2)^{3/2}} \left(\frac{3a_0^2}{a_0^2 + w^2} - 1\right)\right]^{1/2}. \tag{25}$$

The repulsive contact interactions ($q < 0$) give rise to decreasing of the frequency of oscillations compared to the case of pure dipolar interactions ($q = 0$), while the effect of attractive interactions ($q > 0$) is opposite, leading to increasing of the oscillations frequency. In Fig. 2, we depict the frequency of shape oscillations of the soliton as a function of the strength of contact interactions, according to Eq. (25). The same figure shows the stationary width of the soliton for a given strength of contact interactions, obtained from Eq. (24). Comparison between the

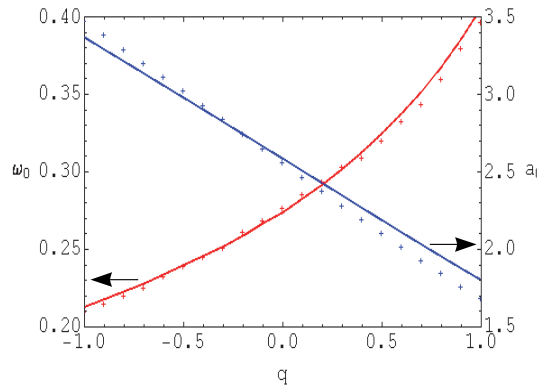

Fig. 2. (Color online) The frequency of low energy shape oscillations (ω_0) of a matter-wave packet in dipolar BEC as a function of the strength of contact interactions q, according to Eq. (25) (red solid line), and the stationary width of the soliton (a_0) obtained from Eq. (24) (blue line). The symbols indicate the results of numerical solution of the GPE (8). Parameter values: $N = 1$, $w = 5$ and $g = 10$.

prediction of VA and the result of numerical solution of the governing GPE (8), expressed by symbols, reveals fairly good agreement.

Low energy collective oscillations of atoms can provide essential information about the interatomic forces in BEC.[28] In this regard, the analytic expression (25) for the frequency of shape oscillations of a matter-wave packet can be useful in relevant experiments with dipolar BEC.

Figure 3 illustrates the oscillations of the soliton's width under periodic variation of the strength of nonlocal interactions. As for the physical implementation of this setting, changing the strength of dipole–dipole interactions can be performed by means of a rotating polarizing magnetic field.[23] Such a field gives rise to precession of dipoles (arranged in "head-to-tail" configuration $\theta = 0$, in a quasi-one dimensional trap) around the axial direction, on a cone of aperture 2ϕ. When the angular frequency of rotation Ω is small than the Larmour frequency, but much greater than the trapping frequencies, only the time average over the period $2\pi/\Omega$ determines the effective strength of dipole–dipole interactions, given by Eq. (2). Thus, by periodic variation of the tilt angle ϕ one can induce the periodic change of the strength of dipolar interactions.

As can be seen in the left panel of Fig. 3, the amplitude of oscillations $(a_{\max} - a_{\min})$ increases linearly at the initial stage, which is characteristic to the resonance phenomenon. Scanning over the interval of frequencies $\omega = 0 - 1$ reveals the parametric resonance at $2\omega_0$ in addition to the main peak at ω_0. To retrieve the width of the wave packet from the solution of the GPE we use the following relation:

$$a(t) = \left(2 \cdot \frac{\int_{-\infty}^{\infty} x^2 |\psi(x,t)|^2 dx}{\int_{-\infty}^{\infty} |\psi(x,t)|^2 dx} \right)^{1/2} . \tag{26}$$

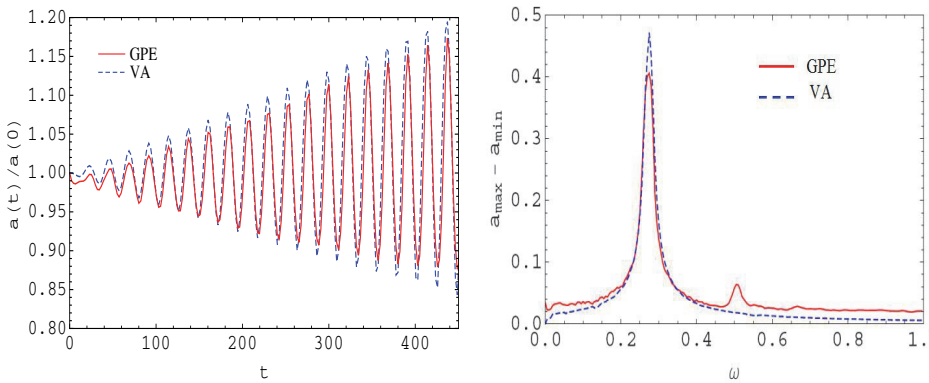

Fig. 3. (Color online) Left panel: Periodic variation of the coefficient of nonlocal nonlinearity $g(t) = 2d^2\alpha(t)$ at resonant frequency $\alpha(t) = 1 + 0.01\sin(\omega_0 t)$, with $d = \sqrt{5}$, $\omega_0 = 0.274$ gives rise to oscillations of the soliton's width. The amplitude of oscillations increases linearly at the initial stage, as characteristic to resonant response. Right panel: Scan over some interval of frequencies $\omega \in [0, 1]$ reveals also the parametric resonance at $\omega \simeq 0.54$, which is the twice of the main resonance frequency ω_0. In both panels, the red solid line corresponds to numerical solution of the GPE (8), while blue dashed line to variational approximation (22). All parameters are the same as in Fig. 1 for pure dipolar interactions.

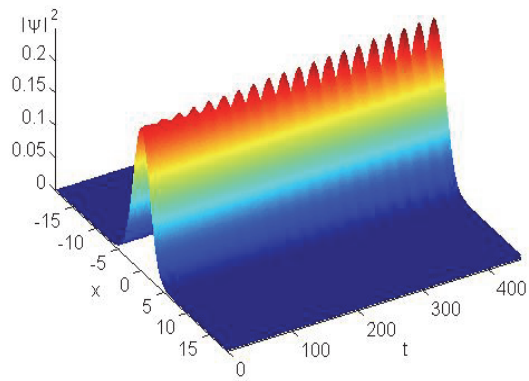

Fig. 4. Evolution of the matter-wave packet under periodic variation of the strength of dipolar interactions. Excitation of shape oscillations under parametric perturbation is evident. The initial condition for the GPE (8) is taken as stationary solution predicted by the variational approximation $\psi(x, 0) = A_0 \exp(-x^2/(2a_0^2))$, with $A_0 = 0.467$ and $a_0 = 2.586$. The coefficient of nonlocal nonlinearity is periodically changed at resonant frequency $\omega_0 = 0.274$ as $g(t) = 10 \cdot (1 + 0.01 \cdot \sin(\omega_0 t))$.

In Fig. 4, we show the evolution of the matter-wave packet under periodically changing coefficient of nonlocal interactions. Excitation of regular oscillations with the frequency of parametric driving is clearly observed. Gradual increase of the amplitude of oscillations is due to the resonance phenomenon.

For numerical simulations of the GPE (8) we employ the split-step method[29] with 1024 Fourier modes in the integration domain $x \in [-6\pi, 6\pi]$. The time step

was set to $\Delta t = 0.001$. To speed up the evaluation of the integral in the nonlocal term, the convolution theorem has been used.[30] It is well known that soliton under perturbation emits linear waves, which can re-enter the integration domain due to reflection from the domain boundaries. For emulation of the infinite integration domain length and preventing the interference of the soliton with the emitted linear waves, we use the absorbing boundary technique.[31]

4. Conclusion

We have studied the effect of atomic dipole–dipole interactions on the dynamics of Bose–Einstein condensates by means of variational approximation and numerical simulations. Dipolar interactions give rise to additional nonlinear term in the Gross–Pitaevskii equation which is spatially nonlocal. For qualitative analysis, we have employed a Gaussian response function in the nonlocal term. The developed model predicts the stationary shape of the soliton in dipolar BEC and its small amplitude dynamics near the equilibrium state quite accurately. Solitons in dipolar BEC exhibit a resonant response to periodic variation of the coefficient of nonlocal nonlinearity at the main perturbation frequency and double of the main frequency, which is characteristic to the phenomenon of parametric resonance. Analytic expression for the frequency of low energy shape oscillations of the matter-wave packet has been derived, which elucidates the contribution of contact and dipolar interactions to the frequency of collective oscillations of the condensate. Obtained results can lead to better understanding of the properties of ultra-cold dipolar quantum gases.

Acknowledgements

This work has been supported by a research grant No. FRGS 0409-108 of the Ministry of Higher Education, Malaysia. B. B. Baizakov is grateful to the Faculty of Science, International Islamic University, Malaysia, for a one month visiting senior fellowship.

References

1. F. Dalfovo, S. Giorgini, L. P. Pitaevskii and S. Stringari, *Rev. Mod. Phys.* **71** (1999) 463.
2. P. G. Kevrekidis, D. J. Frantzeskakis and R. Carretero-González, *Emergent Nonlinear Phenomena in Bose–Einstein Condensates: Theory and Experiment* (Springer-Verlag, Berlin, Heidelberg, 2008).
3. A. Griesmaier, J. Werner, S. Hensler, J. Stuhler and T. Pfau, *Phys. Rev. Lett.* **94** (2005) 160401.
4. T. Lahaye, C. Menotti, L. Santos, M. Lewenstein and T. Pfau, *Rep. Prog. Phys.* **72** (2009) 126401.
5. M. Lu, N. Q. Burdick, S. H. Youn and B. L. Lev, *Phys. Rev. Lett.* **107** (2011) 190401.
6. K. Aikawa, A. Frisch, M. Mark, S. Baier, A. Rietzler, R. Grimm and F. Ferlaino, *Phys. Rev. Lett.* **108** (2012) 210401.

7. S. Kraft, F. Vogt, O. Appel, F. Riehle and U. Sterr, *Phys. Rev. Lett.* **103** (2009) 130401.
8. S. Stellmer, M. K. Tey, B. Huang, R. Grimm and F. Schreck, *Phys. Rev. Lett.* **103** (2009) 200401.
9. R. Ciurylo, E. Tiesinga and P. S. Julienne, *Phys. Rev. A* **71** (2005) 030701; P. Naidon and P. S. Julienne, *ibid.* **74** (2006) 062713.
10. A. Griesmaier, *J. Phys. B: At. Mol. Opt. Phys.* **40** (2007) R91.
11. T. Kohler, K. Goral and P. S. Julienne, *Rev. Mod. Phys.* **78** (2006) 1311; C. Chin, R. Grimm, P. Julienne and E. Tiesinga, *ibid.* **82** (2010) 1225.
12. C. J. Pethick and H. Smith, *Bose–Einstein Condensation in Dilute Gases* (Cambridge University Press, 2002).
13. L. P. Pitaevskii and S. Stringari, *Bose–Einstein Condensation* (Oxford, 2003).
14. P. Pedri and L. Santos, *Phys. Rev. Lett.* **95** (2005) 200404.
15. I. Tikhonenkov, B. A. Malomed and A. Vardi, *Phys. Rev. Lett.* **100** (2008) 090406.
16. J. Cuevas, B. A. Malomed, P. G. Kevrekidis and D. J. Frantzeskakis, *Phys. Rev. A* **79** (2009) 053608.
17. F. Kh. Abdullaev, A. Gammal, B. A. Malomed and L. Tomio, *Phys. Rev. A* **87** (2013) 063621.
18. S. Yi and L. You, *Phys. Rev. A* **66** (2002) 013607.
19. P. A. Andreev, *Mod. Phys. Lett. B* **27** (2013) 1350096.
20. D. Anderson, *Phys. Rev. A* **27** (1983) 1393; B. A. Malomed, *Progr. Opt.* **43** (2002) 69–191.
21. F. Kh. Abdullaev and V. A. Brazhnyi, *J. Phys. B: At. Mol. Opt. Phys.* **45** (2012) 085301.
22. M. Marinescu and L. You, *Phys. Rev. Lett.* **81** (1998) 4596.
23. S. Giovanazzi, A. Görlitz and T. Pfau, *Phys. Rev. Lett.* **89** (2002) 130401.
24. S. Yi and L. You, *Phys. Rev. A* **61** (2000) 041604; K. Goral, K. Rzazewski and T. Pfau, *ibid.* **61** (2000) 051601; L. Santos, G. V. Shlyapnikov, P. Zoller and M. Lewenstein, *Phys. Rev. Lett.* **85** (2000) 1791.
25. S. Sinha and L. Santos, *Phys. Rev. Lett.* **99** (2007) 140406.
26. A. L. Marchant, T. P. Billam, T. P. Wiles, M. M. H. Yu, S. A. Gardiner and S. L. Cornish, *Nat. Commun.* **4** (2013) 1865.
27. M. L. Chiofalo, S. Succi and M. P. Tosi, *Phys. Rev. E* **62** (2000) 7438.
28. D. S. Jin, J. R. Ensher, M. R. Matthews, C. E. Wieman and E. A. Cornell, *Phys. Rev. Lett.* **77** (1996) 420.
29. G. P. Agrawal, *Nonlinear Fiber Optics*, 2nd edn. (Academic Press, New York, 1995).
30. W. H. Press, S. A. Teukolsky, W. T. Vetterling and B. P. Flannery, *Numerical Recipes: The Art of Scientific Computing* (Cambridge University Press, 1996).
31. P. Berg, F. If, P. L. Christiansen and O. Skovgaard, *Phys. Rev. A* **35** (1987) 4167.